Late Inspiral and Merger of Binary Black Holes in Scalar-Tensor Theories of Gravity

James Healy,[1] Tanja Bode,[1] Roland Haas,[2] Enrique Pazos,[3]
Pablo Laguna,[1] Deirdre M. Shoemaker,[1] and Nicolás Yunes[4]

[1]*Center for Relativistic Astrophysics and School of Physics Georgia Institute of Technology, Atlanta, GA 30332*
[2]*TAPIR, California Institute of Technology, Pasadena, CA 91125*
[3]*Departamento de Matemáticas, Universidad de San Carlos, Guatemala, Guatemala*
[4]*Department of Physics, Montana State University, Bozeman, Montana 59717*

Gravitational wave observations will probe non-linear gravitational interactions and thus enable strong tests of Einstein's theory of general relativity. We present a numerical relativity study of the late inspiral and merger of binary black holes in scalar-tensor theories of gravity. We consider black hole binaries in an inhomogeneous scalar field, specifically binaries inside a scalar field bubble, in some cases with a potential. We calculate the emission of dipole radiation. We also show how these configurations trigger detectable differences between gravitational waves in scalar-tensor gravity and the corresponding waves in general relativity. We conclude that, barring an external mechanism to induce dynamics in the scalar field, scalar-tensor gravity binary black holes alone are not capable of awaking a dormant scalar field, and are thus observationally indistinguishable from their general relativistic counterparts.

PACS numbers:

Experimental tests in connection with gravitational redshift, light deflection, Shapiro time delay and perihelion advance, among others, have increased our confidence that general relativity (GR) is the correct theory of gravity [1]. More compelling evidence is provided by binary pulsar observations [2], where the hardening of the binary is accounted for in exquisite detail by one of the fundamental predictions of GR: gravitational wave (GW) emission. Modified gravity theories are nonetheless a possibility [1]. To verify that indeed the podium only belongs to Einstein's theory, strong-gravity tests are needed, involving for instance core-collapse supernovae or the last few orbits and coalescence of compact objects. The new astronomy of GW observations will soon deliver such opportunities, probing gravity at its strongest grip, and thus testing whether Einstein was correct.

In anticipation of GW observations by LIGO, Virgo and other interferometric detectors, exploring what to expect from alternative theories is crucial in assisting data analysis efforts. Of particular importance is the investigation of predictions from alternative theories of gravity during the *generation* of GWs in the non-linear regime. This calls for theoretical studies only accessible with the tools of numerical relativity, which is the focus of the present paper. Among the competing alternatives to GR, scalar-tensor (ST) gravity [3, 4] is one of the most popular due to its simplicity, and because of the motivations provided by string theory scenarios and explanations to dark energy [5]. ST gravity in its simplest form was proposed about a half century ago and is commonly known as Brans-Dicke theory [6].

Studies on observational consequences of ST theories have mostly focused on compact object binaries in the post-Newtonian or extreme-mass-ratio regimes [7–16], a critical prediction of which is the emission of dipole radiation. The latter depends on the sensitivity, s, of the compact objects [1], which is a measure of how susceptible the mass of an object is to variations in the local value of the gravitational constant ($s = 1/2$ for black holes (BHs), and $s \leq 1/5$ for neutron stars [7]). With modifications to GR entering as the difference $\Delta s = s_1 - s_2$ of the binary components, binary black holes (BBHs) are unaffected in ST theories since $s = 1/2$ for all BHs regardless of their masses or spins. For initially stationary scalar fields, Will and Zaglauer [7] proved that BBHs in Brans-Dicke theory are indistinguishable from binaries in GR to first post-Newtonian order. Similarly, Yunes, Pani and Cardoso [16] recently extended this proof to all ST theories and to all post-Newtonian orders, but to leading order in the mass ratio. If the scalar field is not initially stationary, however, Horbatsch and Burgess [17] suggested that BBHs could retain scalar hair [18] and emit dipole radiation, provided the holes have unequal masses.

The goal of the present study is to investigate whether the conclusions from post-Newtonian and extreme-mass ratio studies regarding the BBH indistinguishability between ST and GR theories carries over to the non-linear, comparable-mass regime. Our results confirm this indistinguishability, unless there exists a mechanism to induce dynamics in the scalar field. When the latter activates, the scalar field dynamics triggers dipole energy loss that leads to detectable differences in the '+' and '×' GW polarizations. In the present study, we induce scalar field dynamics by placing the BBHs inside a scalar field bubble, which in some cases includes a potential. These inhomogeneities in the scalar field have a dramatic effect on the BBH dynamics and thus noticeable differences on the GW emission. We show that the changes on BBH dynamics are due to accretion of scalar field by the merging BHs.

We restrict attention to ST theories in vacuum with a

(Jordan frame) action of the form:

$$S = \int \frac{d^4x}{2\,\kappa}\,\sqrt{-\tilde{g}}\left[F(\varphi)\,\widetilde{R} - \zeta(\varphi)\widetilde{\nabla}_\mu\varphi\widetilde{\nabla}^\mu\varphi - 2\,U(\varphi)\right] \tag{1}$$

with $\kappa = 8\,\pi\,G$. Under a conformal transformation $g_{\mu\nu} = F(\varphi)\,\tilde{g}_{\mu\nu}$, or equivalently $\tilde{g}_{\mu\nu} = A^2(\phi)g_{\mu\nu}$, the action (in the Einstein frame) reads [3, 4]:

$$S = \int d^4x\,\sqrt{-g}\,[R/(2\,\kappa) - \nabla_\mu\phi\nabla^\mu\phi/2 - \,V(\phi)] \tag{2}$$

where $(d\phi/d\varphi)^2 = \left[(\zeta/F) + (3/2)(F_{,\varphi}/F)^2\right]/\kappa$ and $V = U/(\kappa\,F^2)$. We set $A(\phi) = e^{a\,\phi - b\,\phi^2/2}$ [3, 4]. Thus, $F = \varphi$ and $\zeta = \omega/\varphi$ with $\omega = -3/2 + \kappa/(a - b\,\phi)^2$. Brans-Dicke theory is recovered when $b = 0$, and GR when $a = b = 0$. We focus here on the case $a = 0$, and consider different values of b.

The Einstein frame is convenient because the action in (2) yields the same equations as those of GR, namely $G_{\mu\nu} = \kappa\,T_{\mu\nu}$ with $T_{\mu\nu} = \nabla_\mu\phi\nabla_\nu\phi - g_{\mu\nu}\,(\nabla_\rho\phi\nabla^\rho\phi/2 + V)$ and $\Box\phi = V_{,\phi}$. Therefore, in the absence of a potential, $\phi = \phi_0 =$ constant yields $G_{\mu\nu} = 0$. Thus, vacuum spacetimes in ST theories will be equivalent to their corresponding spacetimes in GR, independent of the choice of conformal factor $A(\phi)$. This is also the case in the presence of a potential if one arranges for $V(\phi_0) = 0$ and $V_{,\phi}(\phi_0) = 0$. We carried out simulations of spacetimes containing BH singularities that verify this exact equivalence between ST and GR, differing only at the level of round-off errors.

Therefore, the only avenue to trigger differences between ST theories and GR is by inducing dynamics in ϕ. One possibility is with $\partial_t\phi \neq 0$, e.g. $\partial_t\phi = \epsilon\,t$ [17]. Another possibility is by introducing a direct scalar-field curvature coupling to the action, such as $\phi\,R_{\mu\nu\delta\rho}R^{\mu\nu\delta\rho}$ [14, 19] or $\phi\,\epsilon^{\alpha\beta}{}_{\delta\rho}R_{\mu\nu\alpha\beta}R^{\mu\nu\delta\rho}$ [14, 20, 21], that anchors the scalar field to the spacetime curvature. Yet another alternative is by introducing inhomogeneities in ϕ, which is the focus of the present study.

We consider BBH inside a scalar field *bubble* with an initial profile $\phi(r) = \phi_0\,\tanh\left[(r - r_0)/\sigma\right]$ and an inflationary-inspired potential $V = \lambda(\phi^2 - \phi_0^2)^2/8$ that yield discrete symmetry breaking [22]. The bubble has radius r_0, thickness σ, and in the exterior (interior) $\phi = \phi_0\,(-\phi_0)$. Notice that, since we are interested in asymptotically flat spacetimes, $\phi(r \to \infty) = \phi_0$; we shift the conformal factor as $A = e^{-b\,(\phi^2 - \phi_0^2)/2}$, so the Einstein and Jordan frames are both Minkowskian and in the same coordinates [3, 4]. This allows us to make *fair* comparisons between BBHs in ST and GR theories, i.e. comparisons among BBHs with the same BH masses, spins, separation and eccentricity. If $V \neq 0$, the bubble becomes a topologically stable, domain wall with $\sigma \approx 2/(\phi_0\sqrt{\lambda})$ and surface energy density $\mu \approx 3\,\phi_0^3\sqrt{\lambda}/4$ [22]. Since in the interior $V(-\phi_0) = 0$ and $V_{,\phi}(-\phi_0) = 0$, the spacetime in the neighborhood of the BBH can be arranged to be locally, nearly equivalent to its GR counterpart.

Case	ϕ_0	$4\,\pi\lambda/M^2$	M_0/M	M_h/M	a/M_h
A	0	0	0.990	0.952	0.686
B	1/80	0	1.179	0.963	0.688
C	1/40	0	1.747	0.999	0.706
D	1/80	10^3	1.217	0.983	0.685

TABLE I: Parameters, masses and spin.

We discuss results from a set of representative simulations in our study. The simulations were obtained with the MAYA numerical relativity code of our group [23, 24], modified to include the scalar field ϕ in the Einstein frame. In all cases, the binary has non-spinning, equal-mass BHs in quasi-circular orbit, initially separated by $11\,M$, with M the mass of the binary. The bubble surrounding the BBH has a radius $r_0 = 120\,M$ and thickness $\sigma = 8\,M$. The simulations in the Einstein frame differ only in the parameters ϕ_o and λ, as given in Table I. Also in Table I are the values in the Einstein frame of the ADM mass M_0, the mass M_h and spin a/M_h of the final BH. Case A is the reference GR simulation, and D is the only case with non-vanishing potential. Extraction of GWs is carried out in the Jordan frame. For each case, we extract GWs with values $b = 0, 5$ and 10 for the parameter in the conformal factor $A = e^{-b\,(\phi^2 - \phi_0^2)/2}$.

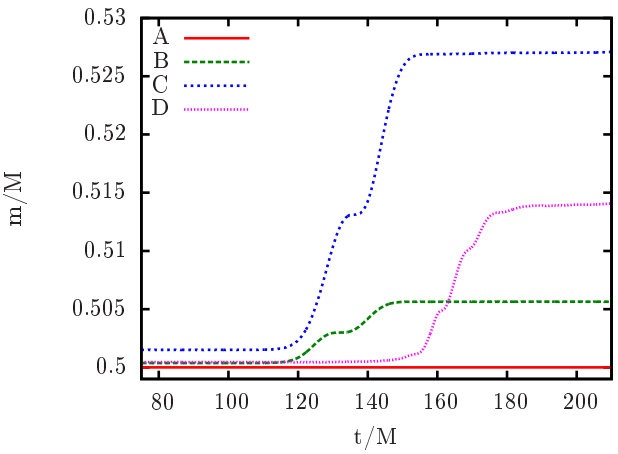

FIG. 1: Mass of the individual BHs as they accrete ϕ before they merge. Here $t = 0\,M$ is the initial time of the simulation.

In all cases, the bubble shell collapses. For case D (a domain wall bubble), the thickness of the shell does not change much during its collapse. For cases B and C with $V = 0$, however, the shell disperses while collapsing. By the time the shell reaches the BBH, the cloud has encompassed the binary. Independent of the details of the initial configuration, the scalar field has a dramatic effect on the BBH dynamics. When the bubble reaches the binary, each BH accretes a significant amount of mass from the scalar field. Figure 1 shows the evolution of the mass (in the Einstein frame) of the individual BHs before they merge. The differences in the initial BH masses among all cases reflect the difficulty of setting up identical bi-

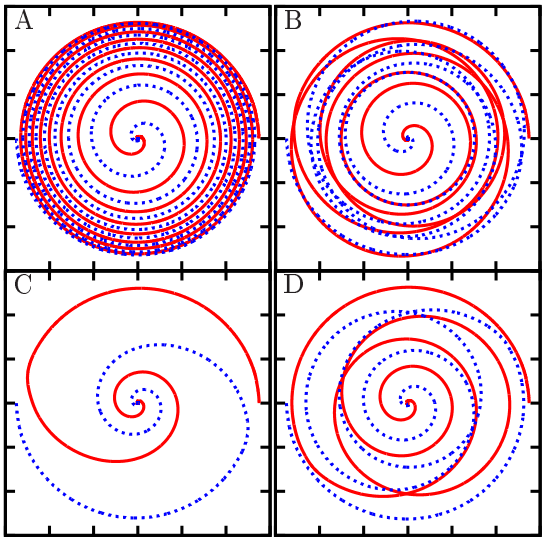

FIG. 2: Trajectories of the BHs when viewed from the Einstein frame.

naries. Notice that for cases B and C the mass increases in two stages. The first increase occurs when the bubble is imploding and passes through the binary. The second increase is after the bubble bounces back and expands. The mass increase in C is larger because the bubble is more massive. With the choice of parameters, the most massive shell is C, followed by D and B (see the ADM mass M_0 in Table I). For case D, the increase in the BH mass as a consequence of ϕ-accretion differs from cases B and C in the presence of multiple step-like increases. This is because in case D the bubble does not just bounce back and dissipate, but instead it lingers in the neighborhood of the binary, bouncing multiple times due to the potential and leading to the series of step increases. Notice that for all cases, the BHs eventually reach a constant mass. The BHs gain 1%, 6% and 3% of their original mass for cases B, C and D, respectively. This gain in mass is correlated with the mass M_h of the final BH. That is, in the GR case A, the final BH is $M_h = 0.952\,M$, while in all other cases and to a good approximation, the final BH mass is $M_h \approx 0.952\,(M + \delta M)$ with δM the mass accreted by the merging BHs, i.e. $0.01\,M$ for B, $0.06\,M$ for C, and $0.03\,M$ for D (see e.g. Table I).

The ϕ-accretion by the BHs has a dramatic effect on the binary dynamics. Figure 2 shows the trajectories (in the Einstein frame) for all cases. Recall that case A is the GR reference case for a BBH in quasi-circular orbit. In all the other cases, the ϕ-bubble induces eccentricity and accelerates the merger. The more massive the shell the larger the induced eccentricity. In particular, for C the influence of ϕ is such that the binary basically plunges.

Not surprisingly, the effect of the bubble is also felt in the emission of gravitational radiation. In Figure 3, we plot the (2,2) mode of the GW strain polarization h_+ (dashed line) and the amplitude $|h| = |h_+ - i\,h_\times|$ (solid line), with $t = 0\,M$ denoting merger time. The strains plotted in panels B, C and D correspond to $b = 0$. Notice the obvious differences between the strains, and in particular when matched against the GR case A. However, within each of the B, C and D cases, the differences between a strain with $b = 0$ and one with $b \neq 0$ are undetectable. That is, the conformal factor does not add new features. We calculated mis-matches between the $b = 0$ and $b \neq 0$ strains for Adv. LIGO, within each B, C and D case, and found them to be $\lesssim 10^{-3}$. This can be understood by studying how the Weyl scalar $\Psi_4 = -C_{l\bar{m}l\bar{m}}$ conformally transforms. The tetrad vectors transform as $\tilde{v}^a = A^{-1}\,v^a$, and the Weyl tensor as $\widetilde{C}_{abcd} = A^2\,C_{abcd}$, and thus $\widetilde{\Psi}_4 = A^{-2}\,\Psi_4 = e^{b\,(\phi^2-\phi_0^2)}\,\Psi_4$ (tilde quantities correspond to the Jordan frame). During the course of the simulation, we observed that the scalar field at the location of the GW extraction behaves as $\phi = \phi_0 + \delta\phi$ with $\delta\phi/\phi_0 \lesssim 10^{-2}$. Therefore, $\widetilde{\Psi}_4 \approx (1 + 2\,b\,\delta\phi\,\phi_0)\,\Psi_4 \approx (1 + 10^{-2}\,b\,\phi_0^2)\,\Psi_4$. Since for the chosen parameters $b\,\phi_0^2 \lesssim 10^{-2}$, $\widetilde{\Psi}_4 \approx \Psi_4$ to one part in 10^4.

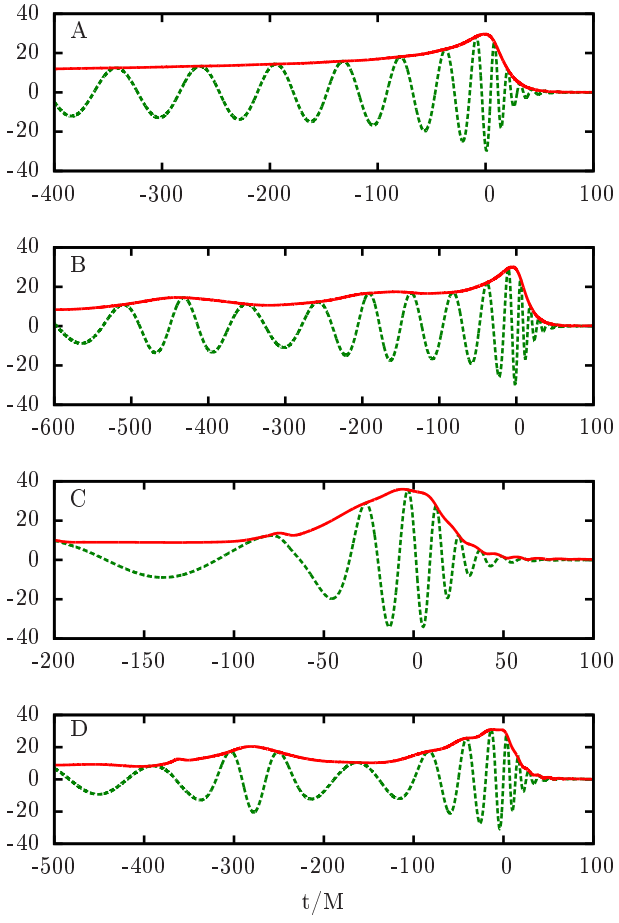

FIG. 3: Mode (2,2) of the gravitational strain $(r/M)\,h_+$ (dashed line) and the amplitude $(r/M)|h| = (r/M)|h_+ - i\,h_\times|$ (solid line). The time $t = 0\,M$ denotes merger time.

In Figure 3, cases B and D show the characteristic strain modulation observed in eccentric BBHs. The

waveform in case C, on the other hand, is basically a burst, since here the binary essentially plunges. Notice also that the amplitudes in C and D show small bumps, the first one at $t \sim -75\,M$ for case C, and at $t \sim -375\,M$ for case D. These bumps are due to the shell as it goes through the binary. The bumps are therefore correlated with the mass jumps in Fig. 1.

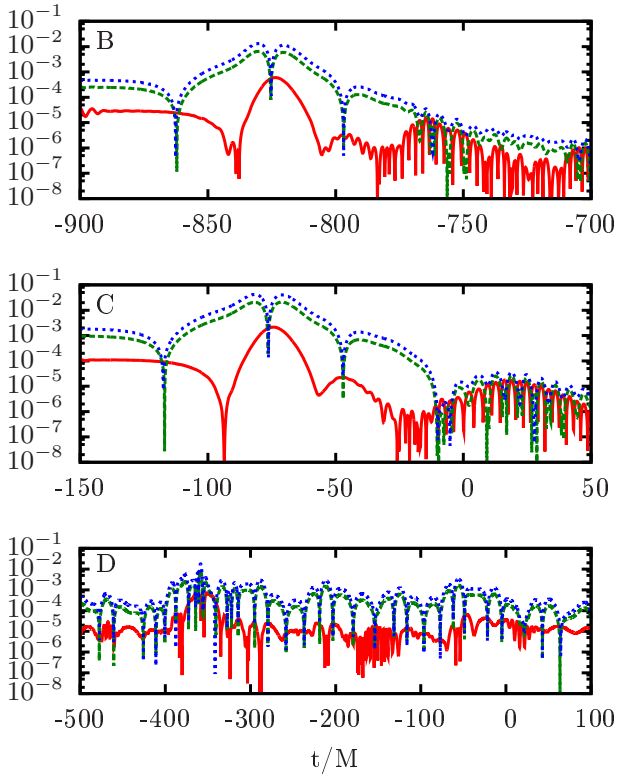

FIG. 4: Mode (0,0) of the breathing mode, $r\,M\,\widetilde{\Phi}_{22}$. In each panel, $b = 0, 5$ and 10 are solid, dashed, and dotted lines, respectively. $t = 0\,M$ denotes merger time.

The presence of a scalar field in ST theories predicts dipole energy losses as well as a new GW polarization, sometimes called a *breathing mode*, given by the traceless Ricci tensor scalar, $\Phi_{22} = -R_{lml\bar{m}} = -R_{ll}/2$ [25, 26]. Figures 4 and 5 show respectively the modes (0,0) and (2,2) of $\widetilde{\Phi}_{22}$ in the Jordan frame. In each panel, $b = 0, 5$ and 10 are solid, dashed, and dotted lines, respectively. The time range in each panel was chosen to highlight when ϕ interacts most strongly with the BHs, with $t = 0\,M$ denoting merger time. The evident b-dependence of $\widetilde{\Phi}_{22}$ can be explained by how $\widetilde{\Phi}_{22}$ conformally transforms: $\widetilde{\Phi}_{2,2} = A^{-2}\,[\Phi_{2,2} + b\,D(\partial_t\phi, \dots)]$, with D a function that vanishes when $\partial_t\phi = 0$. Therefore, at times when ϕ undergoes significant evolution, $\widetilde{\Phi}_{22}$ depends linearly on b, as observed in Figs. 4 and 5. Overlaps of $\widetilde{\Phi}_{22}$ with different b in cases B and C correspond to moments when $\partial_t\phi \approx 0$ at the wave extraction location. Then, as with Ψ_4, one has $\widetilde{\Phi}_{22} \approx \Phi_{22}$. For case D, this does not happen, i.e. $\widetilde{\Phi}_{22}$ with different b values do not overlap because the potential induces longer lived dynamics in ϕ, persisting long after the binary has merged.

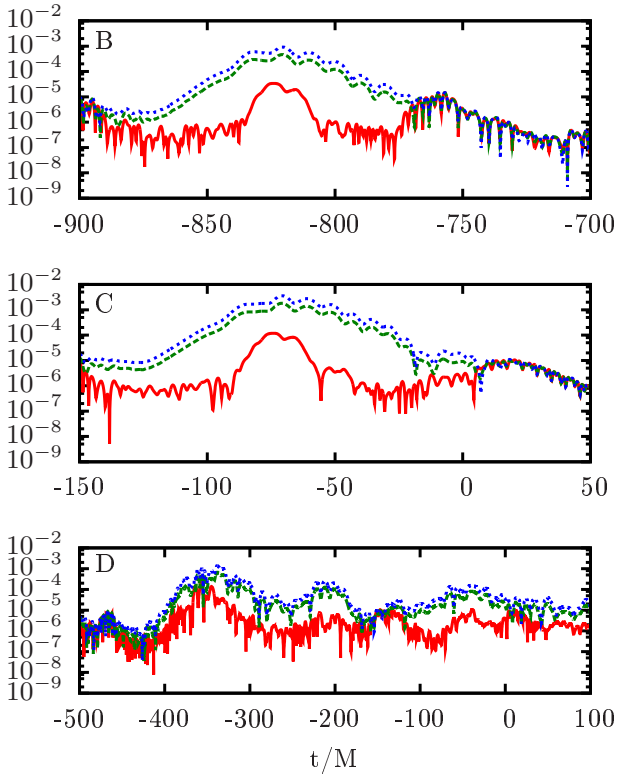

FIG. 5: Same as in Fig. 4 but for the mode (2,2).

This study is a first step towards investigating detectable observational signatures in the GW emission from the late inspiral and merger of a BBH in ST gravity. Our results supports the view that, in order to "defeat" the no-hair constraint of BHs, and thus trigger detectable effects on the gravitational radiation, one needs a mechanism to excite scalar dynamics. In our study, we achieved this with inhomogeneities in the form of a scalar field bubble surrounding the BHs. The effect on the binary was dramatic for the chosen parameters, mostly due to the accretion of scalar field by the merging BHs. In a subsequent study, we will explore a broader range of parameters, particularly those compatible with the parameterized post-Newtonian bounds. We will also consider a situation with a cosmological scalar background, and the inspiral and merger of mixed binary systems.

We thank Cliff Will for fruitful discussions. Work supported by NSF grants 0653443, 0855892, 0914553, 0941417, 0903973, 0955825, 1114374 and NASA grant NNX11AI49G, under sub-award 00001944. Computations at Teragrid TG-MCA08X009 and Georgia Tech FoRCE cluster. RH gratefully acknowledges support by the Natural Sciences and Engineering Council of Canada.

[1] C. M. Will, Living Reviews in Relativity **9** (2006).

[2] J. Taylor, A. Wolszczan, T. Damour, and J. Weisberg, Nature **355**, 132 (1992).

[3] T. Damour and G. Esposito-Farese, Classical and Quantum Gravity **9**, 2093 (1992).

[4] T. Damour and G. Esposito-Farese, Phys. Rev. Lett. **70**, 2220 (1993).

[5] P. Peebles and B. Ratra, Rev. Mod. Phys. **75**, 559 (2003).

[6] C. Brans and R. H. Dicke, Phys. Rev. **124**, 925 (1961).

[7] C. M. Will and H. W. Zaglauer, Astrophys. J. **346**, 366 (1989).

[8] P. D. Scharre and C. M. Will, Phys. Rev. D **65**, 042002 (2002), arXiv:gr-qc/0109044.

[9] K. Yagi and T. Tanaka, Phys. Rev. D **81**, 064008 (2010), 0906.4269.

[10] A. Stavridis and C. M. Will, Phys. Rev. D **80**, 044002 (2009), 0906.3602.

[11] E. Berti, A. Buonanno, and C. M. Will, Classical and Quantum Gravity **22**, 943 (2005), arXiv:gr-qc/0504017.

[12] C. M. Will, Phys. Rev. **D50**, 6058 (1994), gr-qc/9406022.

[13] C. M. Will and N. Yunes, Classical and Quantum Gravity **21**, 4367 (2004), arXiv:gr-qc/0403100.

[14] K. Yagi, L. C. Stein, N. Yunes, and T. Tanaka, ArXiv e-prints (2011), 1110.5950.

[15] J. Gair and N. Yunes, Phys. Rev. D **84**, 064016 (2011), 1106.6313.

[16] N. Yunes, P. Pani, and V. Cardoso, ArXiv e-prints (2011), 1112.3351.

[17] M. W. Horbatsch and C. P. Burgess, ArXiv e-prints (2011), 1111.4009.

[18] T. Jacobson, Physical Review Letters **83**, 2699 (1999), arXiv:astro-ph/9905303.

[19] N. Yunes and L. C. Stein, Phys. Rev. D **83**, 104002 (2011), 1101.2921.

[20] N. Yunes and F. Pretorius, Phys. Rev. D **79**, 084043 (2009), 0902.4669.

[21] S. Alexander and N. Yunes, Physics Reports **480**, 1 (2009), 0907.2562.

[22] G. B. Gelmini, M. Gleiser, and E. W. Kolb, Phys. Rev. D **39**, 1558 (1989), URL `http://link.aps.org/doi/10.1103/PhysRevD.39.1558`.

[23] T. Bode, R. Haas, T. Bogdanovic, P. Laguna, and D. Shoemaker, Astrophys. J. **715**, 1117 (2010), 0912.0087.

[24] F. Löffler, J. Faber, E. Bentivegna, T. Bode, P. Diener, R. Haas, I. Hinder, B. C. Mundim, C. D. Ott, E. Schnetter, et al., ArXiv e-prints (2011), 1111.3344.

[25] D. M. Eardley, D. L. Lee, and A. P. Lightman, Phys. Rev. D **8**, 3308 (1973).

[26] M. E. S. Alves, O. D. Miranda, and J. C. N. de Araujo, Classical and Quantum Gravity **27**, 145010 (2010), 1004.5580.